scientific reports

Check for updates

OPEN

Preoperative brain volume loss is associated with postoperative delirium in advanced heart failure patients supported by left ventricular assist device

Iván Murrieta-Álvarez[1], Jacob P. Scioscia[1], José M. Benítez-Salazar[2], Jason Uwaeze[1,3], Zicheng Xu[3], Guangyao Zheng[3], Shiyi Li[1], Vladimir Braverman[3,4], Carl P. Walther[5], Alexis E. Shafii[1], Camila Hochman-Mendez[6], Todd K. Rosengart[7], Kenneth K. Liao[1] & Nandan K. Mondal[1,6,8]✉

Delirium is a common neurological complication in patients with advanced heart failure (ADHF) following left ventricular assist device (LVAD) implantation, significantly impacting recovery. This study aimed to analyze non-contrast computed tomography (CT) scans of the brain in ADHF patients undergoing LVAD implantation to determine the association between pre-existing brain atrophy and postoperative delirium. A study involving 166 ADHF patients was conducted from March 2020 to July 2023. Non-contrast CT scans were analyzed using advanced quantitative neuroimaging techniques before implantation. The primary marker assessed was the lateral ventricle fraction (LVF), with secondary markers including cortical gray matter fraction (cGMF), white matter fraction (WMF), basal ganglia fraction (BGF), and thalamus fraction (TLF). A total of 56 patients (33%) experienced postoperative delirium within two weeks of implantation. Patients with delirium were older and exhibited greater brain atrophy, indicated by higher LVF and lower cGMF, WMF, BGF, and TLF values. The occurrence of delirium was strongly associated with age, and ventricular enlargement, primarily in the lateral ventricles. LVF effectively predicted delirium development, regardless of age. Preoperative brain volumetric analysis, particularly of the lateral ventricles, may be crucial in identifying patients at risk for postoperative delirium, enhancing postoperative management, and improving outcomes for LVAD recipients.

Keywords Heart failure, Mechanical circulatory support, Delirium, Neurological dysfunction, Brain, Neuroimaging

Advanced heart failure (ADHF) occurs in almost 5% of all hospitalized patients and represents a clinical intersection of therapeutic alternatives that can be utilized depending on the patient's treatment goals and preexisting comorbidities[1]. Durable mechanical circulatory support devices such as left ventricular assist devices (LVADs) have emerged as a vital therapeutic option for patients with ADHF[2], offering significant improvements in quality of life (QoL)[2], acting as a bridge to heart transplantation (BTT) for eligible candidates and adequate circumstances[3], or as a destination therapy (DT). For these reasons, LVADs have become

[1]Michael E. DeBakey Department of Surgery, Division of Cardiothoracic Transplantation and Circulatory Support, Baylor College of Medicine, Houston, TX, USA. [2]Facultad de Medicina, Universidad Popular Autónoma del Estado de Puebla, Puebla, México. [3]Department of Computer Science, Rice University, Houston, TX, USA. [4]Department of Computer Science, Johns Hopkins University, Baltimore, MD, USA. [5]Department of Medicine, Department of Regenerative Medicine Research, Baylor College of Medicine, Texas Heart Institute, Houston, TX, USA. [6]Department of Regenerative Medicine Research, Texas Heart Institute, Houston, TX, USA. [7]Michael E. DeBakey Department of Surgery, Division of Cardiothoracic Surgery, Baylor College of Medicine, Houston, TX, USA. [8]Department of Surgery Cardiothoracic Transplantation and Circulatory Support, Baylor College of Medicine, Texas Heart Institute, Denton A. Cooley Building, 6770 Bertner Avenue, Suite: C928, Houston, TX 77030, USA. ✉email: nandankumar.mondal@bcm.edu

increasingly prevalent[4]. For instance, in 2021, a total of 2464 LVADs were implanted in the United States, and hospitalizations for an implant of these devices are among the most expensive inpatient stays covered by public insurance coverage (Medicare)[5], ranging from 120 000 to 270 000 USD in 2014 and 250 000 and 280 000 USD in 2019[5,6]. Although health expenditure for newer devices is lower[6], longer inpatient stays during index admissions and postoperative recurrent hospitalizations represent an important economic burden. While LVADs have demonstrated remarkable success in prolonging survival, it is essential to recognize that these devices are not without severe complications, such as neurological dysfunction (ND), that could lead to even higher health expenditure, morbidity, and mortality. The Interagency Registry for Mechanically Assisted Circulatory Support (INTERMACS) defines ND as any abnormality related to the central or peripheral nervous system that is attributable to the use of mechanical circulatory support (MCS)[7]. This includes a broad spectrum of neurological events, ranging from temporary neurological impairment (delirium, seizures, or transient ischemic attacks [TIAs]) without structural damage evidence (type 3) to subclinical structural evidence of injury (type 2) to overt ischemic or hemorrhagic strokes (type 1). Prior investigations have indicated that patients undergoing LVAD implantation often present with a prior history of stroke, small vessel cerebral disease (SVCD), manifested as white matter lesions, cerebral microbleeds or brain atrophy, TIAs, and brain tumors[8–10]. The interplay between pre-existing neurological conditions or injuries and the subsequent development of ND in LVAD therapy remains an area of active research. Retrospective registry studies and clinical trials have been valuable sources of information to gauge the incidence, risk factors, and therapeutic alternatives of these complications[11–17]. These studies have offered valuable insights, particularly for patients developing strokes or TIAs as a complication of LVAD therapy, even during the third-generation continuous-flow (CF) LVAD era[12,14]. Nevertheless, there is scant evidence regarding the incidence and impact of other types of ND, perioperative identification, and postoperative resource allocation (frequency of self-care training sessions, inpatient rehabilitation disposition, etc.)[18–21], partly due to a lack of structural and functional quantitative neuroimaging evidence of brain damage before LVAD implants due to the use of preimplant cardiac devices (intra-aortic balloon pump, catheter-based cardiac assist devices), which are MRI incompatible. Nonetheless, evidence suggests that prior neurological damage has an important role in delirium development in postoperative courses[22–24], and MRI-based studies suggest an inconclusive association between the incidence of postoperative delirium in non-cardiac surgery and pre-surgical brain quantitative markers[25–29]. Hence, due to the ongoing use of LVADs as a treatment option for ADHF and the impact of ND, particularly delirium, on inpatient mortality and morbidity during LVAD index admissions, there is a need for reliable biomarkers that can inform clinicians about management strategies for non-vascular ND during heart transplantation and LVAD workup. Leveraging contemporary neuroimaging methods and preliminary data from existing studies, this research aimed to investigate the volume of lateral ventricles as a potential marker of brain parenchymal loss to identify patients at higher risk of experiencing postoperative delirium (type-3 ND) during durable LVAD insertion index admissions.

Methods

Design, patients, and clinical settings

We designed a prospective pilot study to evaluate global and regional brain parenchymal loss performance to discriminate patients developing postoperative delirium (type-3 ND) during the first 30 days after CF-LVAD implantation. We aimed to study brain volumetric markers previously associated with postoperative and ICU-related delirium[22–30] and subcortical structures considered to be vulnerable to global and regional atrophy due to shared and common modifiable and non-modifiable risk factors in LVAD patients, such as advanced age[31–33], obesity[34,35], cardiovascular risk[31,36], prior vascular pathology (small vessel cerebral disease, large vessel occlusion, lacunar strokes, etc.)[36]. In addition, we contemplated the reliability of targeted anatomical structures, considering that they were analyzed using clinical CT scan images. Therefore, we selected the expansion of lateral ventricles (LV) as the primary marker and the decrease of cortical gray matter (cGM), cerebral white matter (WM), thalamus (TL), and basal ganglia (BG) volumes as secondary markers. We sought to study the association of lateral ventricle fraction (LVF) with postoperative delirium incidence and its performance as a biomarker.

A flow diagram depicting the enrollment process is reported in Fig. 1. The study was conducted on 166 ADHF patients with LVAD support at our institution from March 2020 to July 2023. The protocol and consent forms were approved by the Institutional Review Board (H-45532 and H-51123). Patients were screened from the Heart Transplant Program using the following inclusion criteria: (1) Age > 18 years; (2) Advanced heart failure stage NYHA class IV, stage D; (3) Left ventricular ejection fraction (LVEF) ≤ 25%; (4) Inotropic dependency; (5) cardiac index (CI) < 2.2 L/min/m^2 while on inotropes; (6) Medical Review Board and insurance approval for durable LVAD insertion. Patients diagnosed with any form of dementia (Alzheimer's disease, vascular dementia, dementia with Lewy bodies, Parkinson's disease-related dementia, frontotemporal dementia, and mixed dementia) and those not agreeing to participate in the study were excluded from the study. Subjects who underwent an explantation of the device during the study period were eliminated from the research. The primary outcome was defined using the five key features of the American Psychiatric Association's Diagnostic and Statistical Manual, fifth edition (DSM-5)[37]. The DSM-5 criteria for delirium include disturbance in attention and awareness, change in cognition, acute onset and fluctuating course, and evidence of an underlying cause.

Ethics approval

All procedures conducted in studies involving human participants adhered to the ethical standards set forth by the institutional review board at Baylor College of Medicine, with approval granted under protocol numbers H-45532 and H-51123. This research complied with the principles outlined in the 1964 Helsinki Declaration and its subsequent amendments.

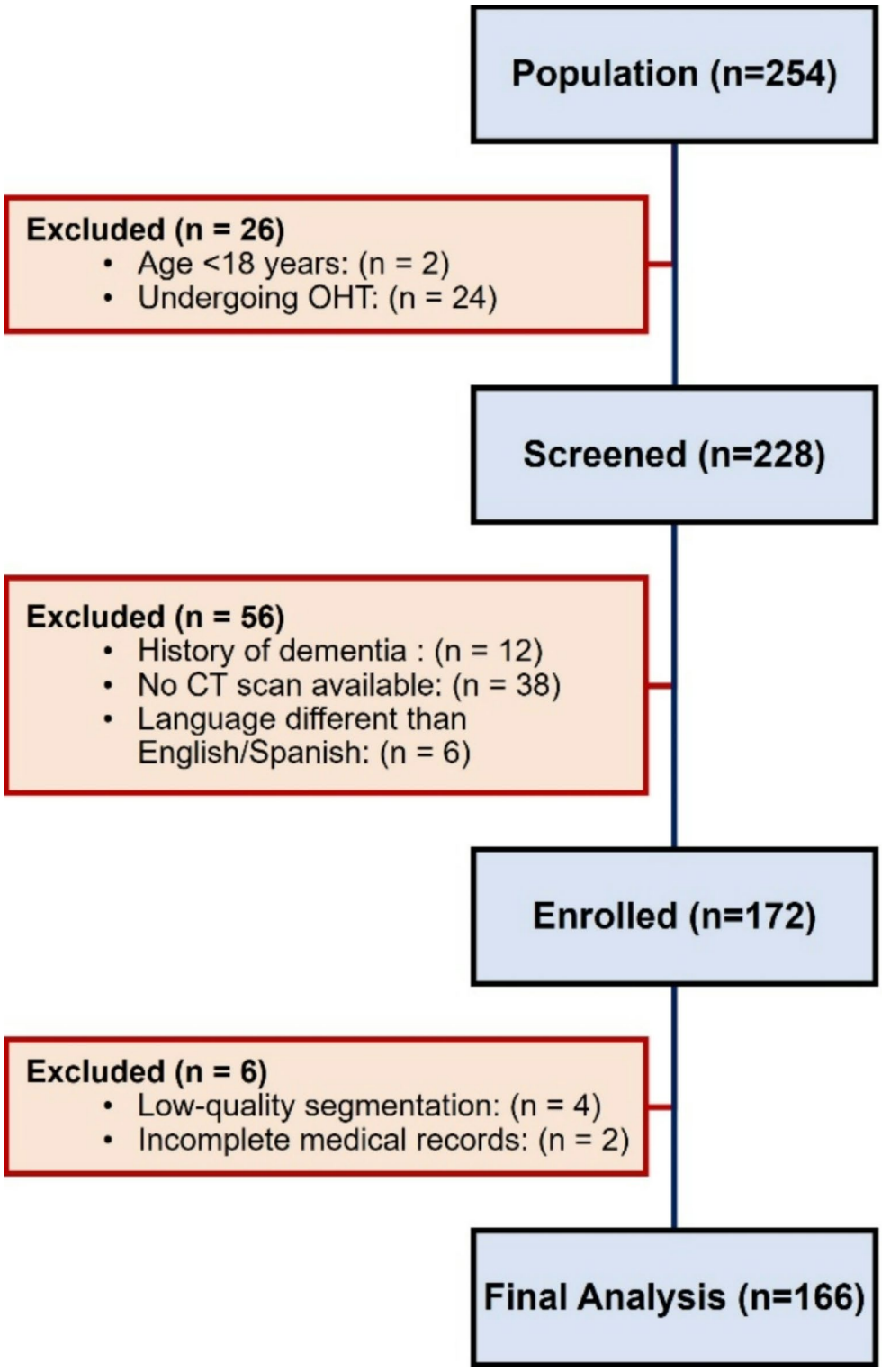

Fig. 1. Flowchart of the study enrollment. Abbreviations: OHT: orthopic heart transplantation; CT: computed tomography.

Consent

In strict adherence to the ethical guidelines outlined in the Federal Policy for the Protection of Human Subjects, also known as 'The Common Rule' (45 CFR 46), and the provisions of the Health Insurance Portability and Accountability Act (HIPAA), informed consent was diligently obtained from each participant enrolled in the study, ensuring compliance with regulatory frameworks governing human subjects' protection and privacy regulations.

Surgical procedure, clinical evaluation, and management

All patients underwent a comprehensive clinical evaluation for heart transplant approval before LVAD insertion. This evaluation included a transthoracic Doppler ultrasound of the heart, a bilateral Doppler ultrasound of the leg and carotid arteries, a pulmonary function test, and a standardized psychosocial assessment conducted by a licensed practitioner. The assessment included the Stanford Integrated Psychosocial Assessment for Transplant (SIPAT)[38], which rates patients from 1 to 120 on readiness and illness management, social support, psychological stability, psychopathology, lifestyle, and the impact of substance abuse. Additionally, the Alcohol Use Disorders Identification Test and CAGE questionnaires were administered if there was a history of substance abuse. A specialized nurse practitioner provided LVAD self-care training for patients. All patients discontinued antiplatelet agents 5 days before the surgery, and warfarin was started on day 5 postoperatively to achieve an International Normalized Ratio (INR) of 2–3. To operationalize the components of DSM-5 into daily evaluations of patients, we utilized the Confusion Assessment Method in the ICU (CAM-ICU)[39] by a trained critical care physician, following institutional protocol. The CAM-ICU is a validated tool specifically designed to detect delirium in ICU patients and aligns well with the DSM-5 criteria since it includes the following components: acute onset or fluctuating course, inattention, altered level of consciousness, and disorganized thinking. Delirium was confirmed through chart review based on dual confirmation by two different assessors using a validated method, achieving an overall agreement of 80% and a kappa of 0.30[40]. Sedation and anesthesia for the surgery were administered using a standardized combination of propofol, fentanyl, dexmedetomidine, isoflurane, and sevoflurane, according to the center's cardiovascular surgery anesthesia management protocol. Patients underwent median sternotomy and mechanical circulatory support (MCS) with cardiopulmonary bypass and anterograde del Nido cardioplegia. Postoperatively, all patients were transferred to the cardiovascular ICU recovery area, where non-pharmacological and pharmacological management of postoperative delirium was initiated. A detailed protocol for managing delirium in the ICU is provided in the online Supplementary Information.

CT scan acquisition and processing

Clinical non-contrast CT scans of the brain were acquired 1 to 5 days before the LVAD implant procedure, using a Siemens® SOMATOM Definition Edge CT scanner. Coronal images were obtained with a slice thickness of 3 mm, and an acquisition matrix of 512×594 pixels was used. The reconstructed images had a diameter of 188 mm and pixel spacing of approximately 0.316 mm in both directions. The scan employed a tube voltage (KVP) of 120 kV and an exposure time of 1000 ms. Radiation exposure parameters indicated a CTDIvol of 43.41 mGy and an estimated dose saving of 22%. The Hounsfield unit (HU) scale was used to rescale the images, and the images were reconstructed with the convolutional kernel Hf38s to allow better gray-white matter differentiation. Coronal images were visually inspected to evaluate artifacts and the overall quality of the images. After being evaluated and selected, de-identified DICOM files were converted to NIfTI files with MRIcron (v1.0.2). The scans were clipped to 0–80 HU; then, we performed symmetric diffeomorphic registration to a stroke-population-specific CT template[41] (Supplementary Information). Brain segmentation was done with a neural network (SynthSeg v2.0) capable of segmenting brain scans of different contrasts and resolutions by using synthetic images generated on the fly and exposing the neural network to random parameters of the generative model, such as resolution, orientation, artifacts, or contrasts[42] (Supplementary Information). Segmentations were visually inspected and manually corrected when appropriate with ITK-SNAP (v4.0.1). Left and right segmentations and volumes obtained from corrected segmentations were fused into one single mask and calculation. Merged segmentations were modeled using spherical harmonization (SPHARM)[43] functions and represented as point distribution models obtaining a parametrically spherical mesh and a surface mesh, and then these models underwent rigid alignment using user-defined reference points to improve the correspondence among SPHARM representations, as implemented in SlicerSALT (v4.0.1). SPHARM average models were displayed in ParaView (v5.13) (Supplementary Information).

Statistical analysis

Descriptive data were analyzed using the Mann-Whitney U or t-test test for continuous variables and chi-squared tests for categorical variables. Data were reported in frequencies and percentages (%) for qualitative data and median and interquartile ranges (IQR) or mean and standard deviation (SD) for quantitative data, as appropriate. Brain metrics not displaying a normal distribution were assessed for different transformations (see Supplementary Figure S1), and the transformation was subsequently used for analyses. We adjusted brain volumes to total intracranial volume (TIV) to account for head size and provide fractional measures of each structure (LVF, cGMF, WMF, TLF, BGF). Then we transformed them into percent to allow better interpretability. Regression models were employed to assess the association of neuroimaging markers with postoperative delirium, using age as a covariate to address confounding. Interaction terms between age and brain volume fractions (LVF, cGMF, WMF, TLF, BGF) were included in subsequent binomial regression models to evaluate the influence of aging on brain atrophy. Due to the lack of prior evidence of postoperative delirium incidence in LVAD patients, we performed simulation-based post hoc sample size and power estimations based on different hypothetical conditions including the simulation of similar conditions proposed in our study ($\rho_1 = 0.45$, $\rho_2 = 0.55$, $a = 0.05$, event ratio 1:3.8 [prevalence 33%]), and assuming that a difference of 0.08 between an area under the curve (AUC) of 0.74 and 0.82 to be clinically relevant in this context (see Supplementary Figure S2). To assess the statistical significance of morphological differences potentially attributed to age, TIV, and comorbidities (including prior stroke history) while considering spatial smoothness, spatial correlation, and low-dimensional representation of functional shape responses, we employed a multivariate functional shaped data analysis (MFSDA) based on a local Wald-type test statistic. The interactions between age and comorbidities were examined in patients with and without delirium, and the results are presented on an average mesh with false discovery rate P-values (*P*-FDR). Diagnostic performance metrics and Wald test chi-squared (χ^2) were

calculated with corresponding 95% confidence intervals (CI). Additionally, F1 scores were calculated to evaluate precision and recall on imbalanced data considering the age groups, and precision-recall curves were plotted. Receiving operating curves (ROC) and the area under the curve (AUC) were calculated and plotted to visualize the performance of LVF in predicting postoperative delirium. We replicated the analyses in a subgroup of patients ≥ 60 years old to assess the association and performance of LVF in identifying postoperative delirium. Additionally, we calculated E-values to provide estimates of the minimum strength of association that an unmeasured confounder would need to have with both the exposure and the outcome to fully explain away the observed association. This approach provides quantitative estimations to contextualize the potential impact of unmeasured clinical factors or perioperative variables on the development of postoperative delirium. The statistical analyses were performed on StataMP (v18.0), R (4.3.2), and SlicerSALT (v4.0.1).

Results

Main features of the sample population

The demographic and clinical characteristics of the study population are displayed in Table 1. The study population consisted of 166 individuals, divided into those who experienced delirium ($n = 56$) and those who did not ($n = 110$). The average age was higher in the delirium group compared to the non-delirium group. The prevalence of type-2 diabetes, and chronic kidney disease (CKD) stage III or higher and white matter hypodensities in NCCT was higher in in the delirium group. Medical history of cortical stroke in the posterior cerebral artery was significantly more common in patients experiencing delirium. Chronic liver disease was less frequently present in the delirium group. Other characteristics showed no significant differences between the groups (Table 1).

Surgical procedure, delirium, and postoperative course

All patients underwent surgery through a median sternotomy and cardiopulmonary bypass (CPB). There were no statistically significant differences in intraoperative variables; however, postoperative outcomes regarding hospital admission length and self-care LVAD training were longer in patients who experienced postoperative delirium (Table 2).

Regional atrophy in patients with and without postoperative delirium

Patients who developed postoperative delirium demonstrated a pronounced expansion of their lateral ventricles, reflecting a significant increase in brain atrophy. This condition was illustrated by an elevated mean lateral ventricular fraction (LVF) (log) (Fig. 2a). In addition to this ventricular enlargement, these patients also exhibited notable reductions in the volume of various types of parenchymal tissue. Specifically, there was a marked decrease in the volume of cortical gray matter (Fig. 2b), white matter (Fig. 2c), basal ganglia (Fig. 2d), and the thalamus (Fig. 2e). All these changes serve as indicators of increased brain atrophy. The differences in brain tissue volumes were statistically significant and ranged from moderate to large, with Cohen's d estimates between 0.5 and 0.9. Among these, the most substantial changes were observed in the LVF. Interestingly, when focusing on patients aged over 60, only the LVF (log) (Fig. 2f) and white matter (Fig. 2g) remained significantly different from those without delirium, while no such differences were evident for gray matter (Fig. 2h), basal ganglia (Fig. 2i), and the thalamus (Fig. 2j). Even in these older patients, the difference in LVF was particularly pronounced, maintaining its categorization as a large effect.

Association between postoperative delirium with age and regional brain atrophy

To understand and estimate the influence of age on subcortical atrophy and the occurrence of postoperative delirium, we fitted different linear models using age as a predictor of lateral ventricles expansion. We noted that patients with and without postoperative delirium displayed a significant association of age with LVF (log) (Fig. 3a) and LVF (%) (Fig. 3b). However, no linear associations were found in patients with or without postoperative delirium between age and LVF (Fig. 3c and d).

Ventricular shape morphology in patients experiencing postoperative delirium

The average mesh representation of the fused lateral ventricles, reconstructed using Spherical Harmonic Analysis for the Representation of Morphology (SPHARM) presented in Fig. 4. The statistical shape model of fused lateral ventricles met the spherical assumption and revealed significant insights into the relationship between ventricular morphology and age in patients experiencing postoperative delirium. The multivariate functional shape data analysis (MFSDA) modeling demonstrated that there was a significant relationship between years of age and ventricular expansion only in patients who experienced postoperative delirium. Older patients exhibited greater ventricular enlargement and shape deformation than younger patients. Vertex variations in the shape model highlighted specific regions of the ventricles, predominantly at the body (central region), where these deformations were most pronounced, with FDR P-values (< 0.05) displayed in red on an average mesh, providing a detailed map of age-related morphological changes (Fig. 4). Patients without postoperative delirium did not show any significant association with vertex variations.

Association between brain volumetrics, clinical factors, and postoperative delirium

Table 3 demonstrates a significant correlation between various brain volumetric markers and the occurrence of postoperative delirium. Notably, LVF demonstrated a strong association with postoperative delirium in the overall patient cohort and patients over 60 years old. Similarly, cGMF, WMF, and TLF were associated with the incidence of postoperative delirium. However, the just LVF (log) remained significantly associated in patients > 60 years old. While BGF and TLF showed significant associations in unadjusted models, these associations lost significance after adjustment (Table 3). The models aimed to evaluate the influence of age on

	All ($n=166$)	Delirium ($n=56$)	No Delirium ($n=110$)	*P*-value
Male	133 (80)	48 (86)	85 (77)	0.198
Age, *years*	59 (SD 13)	63 (SD 12)	57 (SD 13)	**0.001***
BMI, kg/m^2	26 (IQR 23–30)	27 (IQR 23–30)	26 (IQR 23–30)	0.671
Self-reported ethnicity				0.798
Black	70 (42)	24 (43)	46 (42)	
White	65 (39)	21 (38)	44 (40)	
Hispanic/Latino	27 (16)	9 (16)	18 (16)	
Asian	3 (2)	2 (3)	1 (1)	
Native Hawaiian/Pacific Islander	1 (1)	0 (0)	1 (1)	
Cardiomyopathy etiology				0.080
Non-ischemic cardiomyopathy	84 (49)	23 (41)	61 (56)	
Ischemic cardiomyopathy	82 (51)	33 (59)	49 (44)	
Device				0.099
Heartmate 3™	109 (66)	32 (57)	77 (70)	
HeartWare™	57 (34)	24 (43)	33 (30)	
Therapy intention				**0.043***
DT	149 (90)	54 (96)	95 (87)	
BTT	17 (10)	2 (4)	15 (13)	
INTERMACS Profile				0.922
1	12 (7)	3 (5)	9 (8)	
2	76 (46)	25 (45)	51 (47)	
3	69 (42)	25 (45)	44 (40)	
4	8 (4)	3 (5)	5 (4)	
5	1 (1)	0 (0)	1 (1)	
Temporary MCS before implant[a]	102 (61)	32 (57)	70 (63)	0.390
IABP	61 (37)	18 (32)	43 (39)	0.425
Impella® CP, 5 and 5.5	33 (20)	12 (21)	21 (19)	0.680
ECMO	8 (5)	2 (4)	6 (5)	0.719
6MWD, *m*	218 (IQR 89–307)	204 (IQR 83–301)	221 (IQR 75–297)	0.328
SIPAT score	5 (IQR 1–11)	6 (IQR 1–11)	5 (IQR 1–10)	0.463
Hearing impairment	43 (26)	16 (28)	27 (24)	0.557
Recent history of drug abuse	27 (16)	9 (16)	18 (16)	0.874
Type-2 diabetes	95 (57)	40 (71)	55 (50)	**0.008***
History CKD stage ≥ III	114 (69)	47 (84)	67 (61)	**0.003***
Atrial fibrillation	83 (50)	32 (57)	51 (47)	0.189
Chronic liver disease	18 (11)	2 (4)	16 (14)	**0.032***
Peripheral vascular disease	26 (16)	12 (21)	14 (13)	0.145
COPD	27 (16)	10 (18)	17 (16)	0.692
Prior stroke	42 (25)	16 (29)	26 (24)	0.489
Cortical stroke	33 (20)	14 (25)	19 (17)	0.472
Vascular territories of cortical strokes				
ACA	4 (2)	0 (0)	4 (4)	0.267
Left	2 (1)	0 (0)	2 (2)	0.696
Right	2 (1)	0 (0)	2 (2)	0.427
MCA	24 (14)	10 (18)	14 (13)	0.818
Left	11 (7)	5 (9)	6 (5)	0.823
Right	14 (8)	5 (9)	9 (8)	0.909
PCA	8 (5)	6 (11)	2 (1)	**0.047***
Continued				

	All ($n=166$)	Delirium ($n=56$)	No Delirium ($n=110$)	*P*-value
Left	5 (3)	4 (7)	1 (1)	0.117
Right	3 (2)	2 (4)	1 (1)	0.659
Lacunar infarcts	8 (5)	2 (4)	6 (5)	0.657
White matter hypodensities	72 (43)	32 (57)	40 (36)	**0.016***
History of neurological comorbidity[b]	54 (33)	21 (38)	33 (30)	0.329

Table 1. Clinical and demographic characteristics of the study population. Abbreviations: BMI, body mass index; DT, destination therapy; BTT, bridge-to-transplant; INTERMACS, Interagency Registry for Mechanically Assisted Circulatory Support; MCS, Mechanical circulatory support; IABP, Intraaortic balloon pump; ECMO, extracorporeal membrane oxygenation; SIPAT, Stanford Integrated Psychosocial Assessment for Transplant; CKD, Chronic kidney disease; COPD, Chronic obstructive pulmonary disease; ACA, anterior cerebral artery; MCA, middle cerebral artery; PCA, posterior cerebral artery. Quantitative data are summarized in mean and standard deviation (SD) or median and interquartile range (IQR), according to its distribution. Categorical data is summarized in absolute frequency and percentages (%). [a] IABP, Impella or ECMO. [b] Traumatic brain injury, seizure disorder, movement disorder or stroke. *Denotes *P*-value < 0.05

	All ($n=166$)	Delirium ($n=56$)	No Delirium ($n=110$)	*P*-value
Use of aortic clamp	67 (40)	20 (36)	47 (42)	0.537
Aortic clamp time, *min*	36 (19–41)	38.5 (15.7–50.5)	34 (21.5–40.5)	0.235
Cardiopulmonary bypass time, *min*	74 (58–103)	80 (60–106.5)	72.5 (58–101)	0.327
Mediastinal washout	26 (16)	11 (20)	15 (14)	0.406
Time to start of self-care LVAD training, *days*	8 (6–13)	9 (7–22.7)	8 (6–12)	0.115
Completed self-care LVAD training[a]	89 (61)	21 (43)	68 (69)	**0.016***
Duration of self-care LVAD training[b]	12 (7–19)	16.5 (9.2–22)	11 (7–16)	**0.001***
ICU length of stay, *days*	15 (11–27)	16.5 (13–31)	15 (10–25)	**0.016***
Postoperative length of stay, *days*	25 (17–35)	32 (20–53.5)	22.5 (16–32)	**< 0.001***
Overall admission length, *days*	41 (29–54)	48 (34–72)	36 (28–51.7)	**0.003***
In-hospital deaths	19 (11)	8 (14)	11 (10)	0.546

Table 2. Perioperative characteristics and operative and admission outcomes. Abbreviations: LVAD, left ventricular assist device; ICU, intensive care unit; Min, minutes Quantitative data are summarized in mean and standard deviation (SD) or median and interquartile range (IQR), according to its distribution. Categorical data is summarized in absolute frequency and percentages (%). [a] Excluded patients who died during admission. [b] Excluded patients who did not start the self-care LVAD training. *Denotes *P*-value < 0.05

LVF and postoperative delirium indicated similar results (Table S1). The interaction between age and LVF did not yield significant results in the overall patient cohort (OR 1.30; 95% CI 0.16–4.34; $P=0.099$). Similar findings were observed in patients over 60 years old (OR 0.98; 95% CI 0.86–1.50; $P=0.741$) (Table S1).

Further analysis to identify the association between modifiable and non-modifiable risk factors and postoperative delirium is presented in the online supplemental information (see Supplementary Table S2 and Table S3). We noticed that a history of type-2 diabetes was significantly associated with postoperative delirium in the unadjusted and adjusted model in all patients (Table S2), and this association remained significant in the unadjusted and adjusted model of patients > 60 years old (see Supplementary Table S3). Similarly, the unadjusted model for CKD stage ≥ III history showed a significant association with postoperative delirium. This association remained significant in the adjusted model (**Table S2**). In patients > 60 years old, history of CKD stage ≥ III was not significantly associated in unadjusted and adjusted models (see Supplementary Table S3).

The evaluation of unmeasured confounders using E values revealed that an unmeasured variable would need to be associated with the outcome (postoperative delirium) with an OR between 4.82 and 5.46 to invalidate the association between LVF (log) and postoperative delirium. Furthermore, an OR between 5.64 and 5.68 would be necessary to completely explain away the association of LVF (log) with postoperative delirium in patients over 60 years of age (Table S4).

Baseline LVF in identifying patients at risk for postoperative delirium

We used age-adjusted logistic models to assess the effectiveness of baseline LVF in identifying patients at risk for postoperative delirium. Our results showed that LVF (log) performed well in all cohorts (Fig. 5a) and in patients over 60 years old (Fig. 5c), with minimal differences in AUC. Similarly, LVF (%) adjusted for age effectively distinguished patients with postoperative delirium in the overall group (Fig. 5b) and those over 60 (Fig. 5d), also

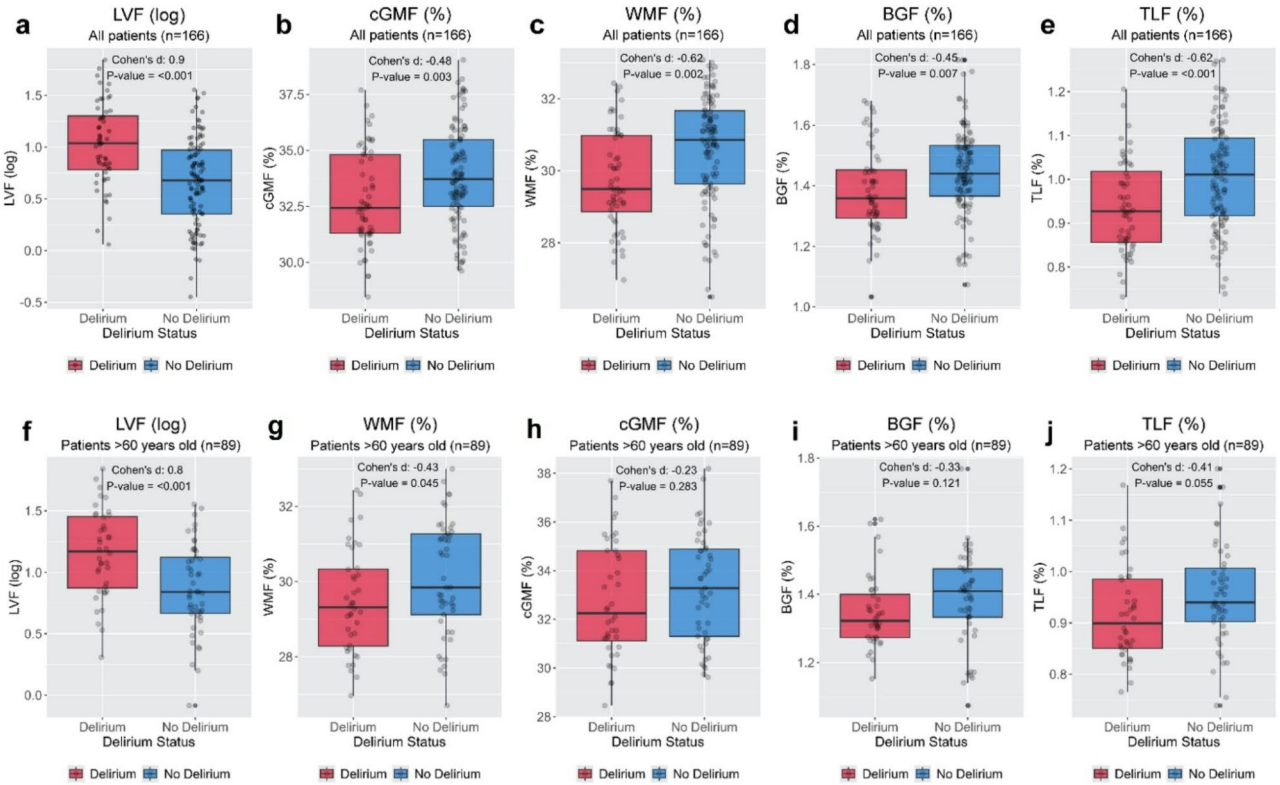

Fig. 2. The plots illustrate the comparisons of five brain volume metrics: LVF, cGMF, WMF, BGF, and TLF in all patients of the cohort (**a** through **e**) and in patients > 60 years old (**f** through **j**) with and without postoperative delirium. Each plot highlights the differences in mean and median values between the two groups, showing higher ventricular expansion in all patients and those > 60 years old. Abbreviations: LVF, lateral ventricular fraction; cGMF, cortical gray matter fraction; WMF, white matter fraction; BGF, basal ganglia fraction; TLF, thalamus fraction.

showing minimal AUC differences. Additional metrics, including sensitivity and specificity, are available in the online supplemental information (see Supplementary Table S3).

Discussion

Our study quantitatively analyzed clinical non-contrast CT scans of the brain in ADHF patients undergoing LVAD insertion to determine the association between preexisting brain atrophy and postoperative delirium, and its adequacy in identifying at-risk patients before surgery. Our findings suggest that pronounced brain parenchymal loss, indicated by a higher LVF at the time of LVAD implantation, is associated with an increased incidence of postoperative delirium, regardless of age. Age is one of the most significant factors driving delirium after both cardiac[44–46] and non-cardiac surgery[47,48]. Additionally, we observed that the age-adjusted LVF reasonably predicts the incidence of postoperative delirium. WM, cortical GM, and subcortical GM atrophy were significantly lower in patients experiencing postoperative delirium, consistent with previous reports with similar findings[22,23,26,27]. However, these differences were slightly smaller compared to the changes observed with the LV. We propose that the expansion of the LV observed in patients with delirium is substantial and strongly associated with the condition. Although this expansion cannot be precisely attributed to either gray or white matter, its significance is evident. Our study did not reveal statistically significant associations between parenchymal volumetric estimations (cGMF, WMF, BGF, TLF) and postoperative delirium in patients over 60. However, there is an indication of an atrophying effect, which may be partially mitigated by employing synthetic images derived from low-resolution CT scans to quantify volumes (segmentation of CSF tends to be more precise in comparison with gray and white matter structures). Notably, in the entire cohort, cGMF, WMF, and TLF were associated with postoperative delirium. This suggests that cortical and subcortical atrophy, consistent with the expansion of the lateral ventricles, is a significant factor in the development of delirium.

Furthermore, the role of age on LV expansion, as shown by morphological differences in age-shape associations and the incidence of delirium, appears to be prominent. This indicates that not only is the overall change in cerebral mass tissue relevant, but also the pattern of morphological shifts accompanying this process in the development of postoperative delirium.

These findings resembled the behavior of age over the structural integrity of brain structures previously reported in healthy and diseased individuals[31,36], suggesting that the baseline structural integrity of the brain is highly related to the incidence of ND in ADHF patients undergoing LVAD insertion. Even though age was

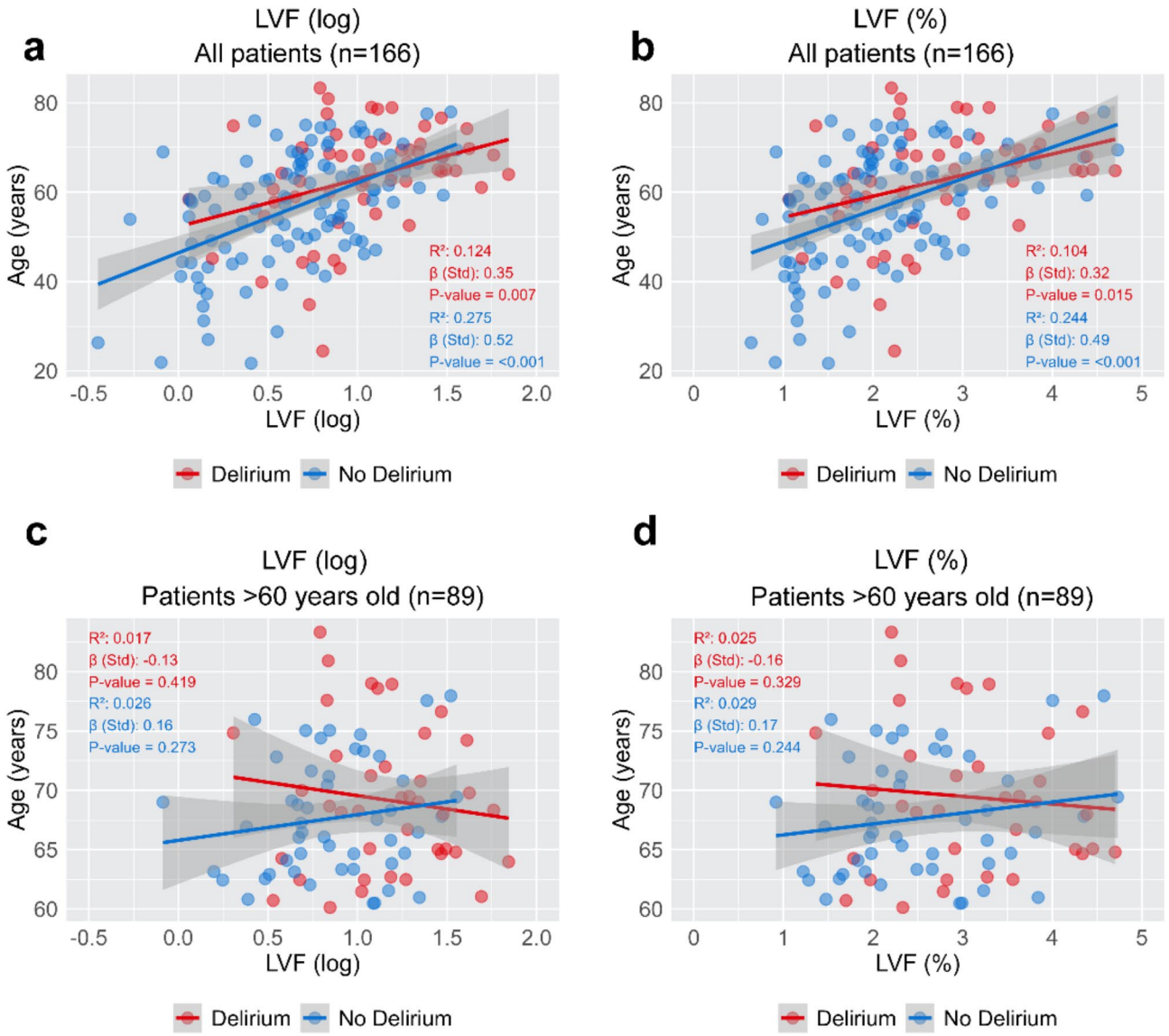

Fig. 3. Scatter fit plots demonstrate the relationship between age and log-transformed LVF (**a**) and LVF percentage (**b**) in the entire patient cohort. Additionally, they show the relationship between age and log-transformed LVF (**c**) and LVF percentage (**d**) in patients over 60 years old. Significant associations are observed between age and LVF in the overall cohort; however, no significant associations are found in patients over the age of 60. Abbreviations: LVF, lateral ventricles fraction. Estimates and parameter descriptions.

the main driver of brain atrophy and postoperative delirium, we suspect that additional factors such as prior cumulative cerebrovascular injury (sustained brain hypoperfusion, cardiorenal syndrome, long-standing hypertension, etc.) over the CNS and the surgical procedure itself (systemic inflammation, pump use, transient hypo- hypervolemia, and prolonged ventilation) are two additional factors involved in the development of postoperative delirium in these circumstances. This could be partially supported by prior studies using multimodal neuroimaging describing the effect of high cardiovascular risk and pre-established macro and microstructural brain injury[30,33,36].

We believe that patients in our study with more pronounced brain atrophy were in the later stages of SVCD[49]. Preoperative MRI studies in patients undergoing cardiac surgery have shown that larger ventricular volumes, new ischemic lesions, and white matter disease (deep subcortical white matter and periventricular hyperintensities) are linked to postoperative delirium[21,22,50]. This suggests that in the earlier stages of ischemic cardiomyopathy before LVAD implantation, the brain might have structural abnormalities that increase the risk of postoperative delirium due to CNS injuries, such as blood-brain barrier (BBB) disruption[51–53]. Studies on patients undergoing on-pump cardiac and non-cardiac surgery have shown that postoperative BBB disruption, assessed through CSF enhancement (hyperintense acute reperfusion marker or HARM) in FLAIR sequences or contrast extravasation subtraction, correlates significantly with lesions on diffusion-weighted images[54] and

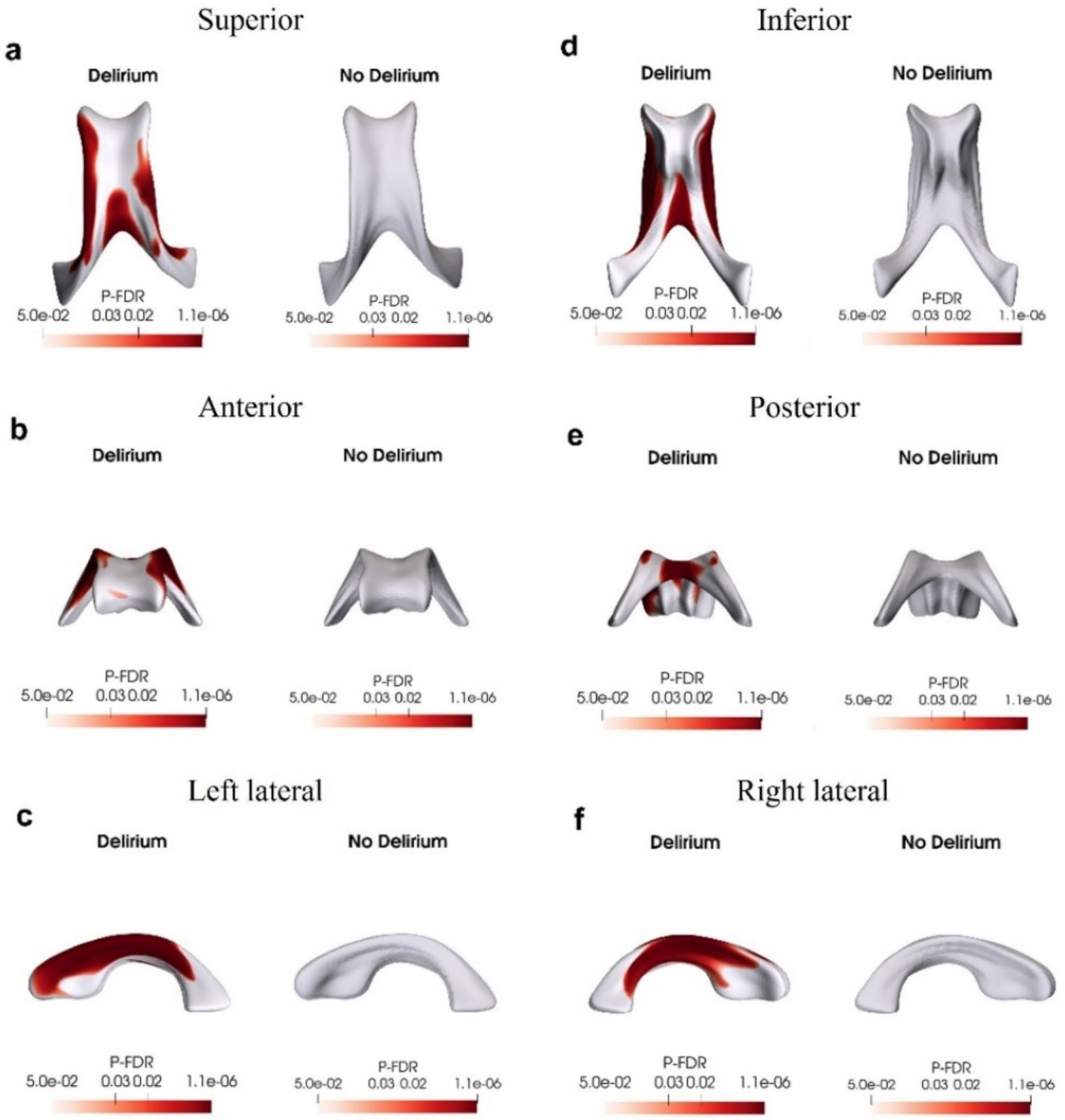

Fig. 4. Average mesh representations of the fused left ventricle (LV) are displayed in six standard anatomical views: superior (**a**), anterior (**b**), left lateral (**c**), inferior (**d**), posterior (**e**), and right lateral (**f**). Red clusters in the figure indicate significant surface expansion in patients with postoperative delirium compared to those without, following a Bonferroni correction for multiple comparisons. These clusters highlight the association of expansion with age, suggesting that brain atrophy is more pronounced in older patients with postoperative delirium. Open-source software SlicerSALT (https://salt.slicer.org/) and Paraview (https://www.paraview.org/) were used to generate Fig. 4.

cognitive function[51]. Additionally, BBB disruption, indicated by CSF enhancement, has been associated with advanced age, cerebral microbleeds, and brain atrophy[55], which are part of the SVCD spectrum.

Findings from the present study might support the use of clinical non-contrast brain CT scans enhanced by the generation of synthetic images to assess the risk of ND in patients undergoing LVAD implantation. Due to the varying availability and LVAD-compatibility of brain MRI, non-contrast CT scans present a promising alternative for quantitative analyses by (1) providing objective evidence of neurological risk for postoperative management and (2) utilizing an imaging exam commonly performed in ADHF patients to rule out cerebrovascular disease,

All patients ($n = 166$)				
	Unadjusted		Adjusted	
Brain marker	OR (95% CI)	*P*-value	OR (95% CI)	*P*-value
LVF (log)	9.04 (3.78–24.0)	**< 0.001***	7.63 (2.89–22.24)	**< 0.001***
cGMF	0.79 (0.67–0.92)	**0.004***	0.84 (0.71–0.99)	**0.045***
WMF	0.66 (0.52–0.83)	**< 0.001***	0.72 (0.56–0.92)	**0.011***
BGF	0.04 (0.003–0.41)	**0.008***	0.15 (0.01–2.14)	0.169
TLF	0.004 (0.0001–0.08)	**< 0.001***	0.01 (0.0004–0.45)	**0.011***
Patients > 60 years old ($n = 89$)				
	Unadjusted		Adjusted	
Brain marker	OR (95% CI)	*P*-value	OR (95% CI)	*P*-value
LVF (log)	9.70 (2.75–40.78)	**< 0.001***	9.65 (2.70–41.20)	**0.001***
cGMF	0.90 (0.74–1.08)	0.277	0.91 (0.75–1.10)	0.371
WMF	0.74 (0.54–0.99)	0.051	1.04 (0.96–1.13)	0.074
BGF	0.06 (0.001–2.11)	0.133	0.10 (0.002–3.90)	0.227
TLF	0.01 (0.0009–1.07)	0.062	0.02 (0.0001–2.04)	0.108

Table 3. Association between brain volumetrics and postoperative delirium. Abbreviations: LVF, lateral ventricles fraction; cGMF, cortical gray matter fraction; WMF, white matter fraction; BGF, basal ganglia fraction; TLF, thalamus fraction. The adjustment of models employed age as a covariate. *Denotes *P*-value < 0.05

a "strongly adverse factor" for heart transplant according to Medicare coverage rules[56]. Notably, a significant proportion of patients in our study had central lines or probes inserted on the right side of the neck before surgery, preventing a complete internal carotid artery (ICA) Doppler ultrasound to identify carotid stenosis, a recognized postoperative delirium risk factor[50,57], and a test included in the stroke, transient ischemic attack (TIA), and carotid dissection workup. Similarly, pre-implant neuropsychological evaluations[58–61] that could aid in estimating delirium risk cannot be easily or reliably performed in ventilated, sedated, or extremely fatigued patients, which could occur in up to 30–40% of patients, particularly those with INTERMACS profile I to II[62]. Identifying at-risk patients for postoperative delirium is crucial for anticipating strategies to manage cognitive demands after LVAD implantation, improving LVAD self-care training proficiency, identifying overlapping ND, shortening length of stay (LOS), and preventing complications. We believe that the quantification of brain volumetrics using synthetic-based imaging pipelines, along with the application of normalized metrics (such as z-scores) derived from multicenter validation studies, holds significant promise for implementing this intervention in patients undergoing LVAD workup.

Although these observations hold significant clinical implications, we must acknowledge the limitations of our study. First, this is a single-center observational study without a control group and with a relatively small sample size, which introduces selection bias, temporality issues, and reverse causality, potentially challenging the establishment of causal relationships, and even though the estimations of unmeasured confounding showed that the findings regarding lateral ventricular expansion would need considerably large effect sizes from unmeasured confounders, such as, acute renal dysfunction, oxygenation or hemodynamic instability to discard the observations, the conclusions should be carefully interpreted. Importantly, slightly different acquisition protocols of brain imaging from different eras could disrupt the localization of anatomical structures and result in large differences in volumetric estimations. Additionally, the sample size for the subanalyses in patients > 60 years old was smaller than the original cohort, therefore the estimations provided by those models are not powered for the study's main hypothesis. Another issue with imaging acquisition arises from the varying times and days when CT scans were obtained, as lateral ventricle volume changes throughout the day and under different circumstances. Additionally, we did not perform neuropsychological testing to obtain quantitative metrics for cognitive performance before surgery. Using non-contrast CT brain scans with 3-mm resolution is also suboptimal for conventional quantitative neuroimaging analyses due to partial low resolution and problematic gray-white matter differentiation in some individuals, potentially omitting subtle structural details. We employed a 3D deep learning method to segment brain scans; however, 3D segmentation models might be sensitive to the misalignment of medical images and require high computational resources. These limitations could be mitigated using a 2D segmentation method, which decreases image coregistration dependencies and computational load. To address these limitations, we employed a robust deep-learning network to register prior brain lesions in MRI and CT brain scans and generate synthetic images with considerable precision. Furthermore, the enrollment of patients in our study was inclusive enough to provide a representative sample with characteristics partially similar to those in multicenter registries and clinical trials[3,4].

Insights from this preliminary work pave the way for further studies on the structural integrity of the CNS in patients with acute decompensated heart failure, both young and old, as well as those with ischemic cardiomyopathy (ICM) and non-ischemic cardiomyopathy (NICM). Initially, robust deep learning algorithms can be employed to analyze neuroimaging data acquired for clinical purposes, such as ruling out cerebrovascular disease, to study ND in a population with diverse risk levels. Additionally, segmentation and generation of synthetic scans from native non-contrast clinical CT scans of the brain could provide valuable insights into

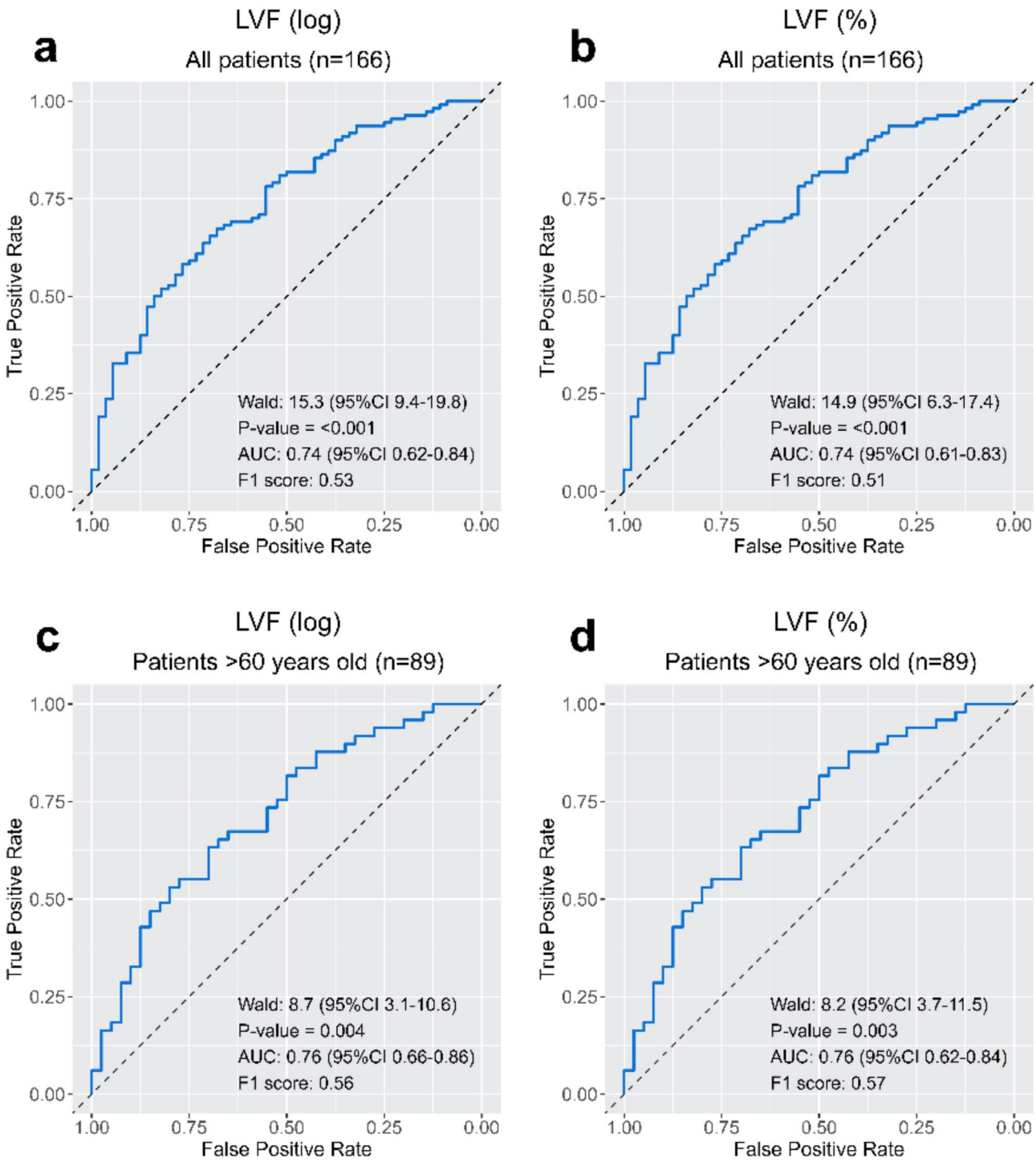

Fig. 5. ROC curves showing the classification, precision, and recall performance of age-adjusted LVF as a predictor for postoperative delirium in all the cohorts employing LVF (log) (**a**) and LVF (%) (**b**), and LVF (log) (**c**) and LVF (%) (**d**) in patients age > 60 years old.

the association between CNS structural integrity and postoperative outcomes, offering alternatives to improve resource utilization. Prospective multicentric studies with larger sample sizes from different centers and varied CT acquisition protocols are needed to address the lack of generalizability of these findings, validate the performance of this biomarker, and provide reliable normative metrics in this population. These iterations will help to answer whether the preoperative characterization of brain structural integrity might offer a new understanding of the current ND classification by INTERMACS or help to tailor individual ND risks and management strategies (sedation protocols, training planning, etc.) for postoperative delirium, TIAs, and strokes. Consequently, these observations might provide valuable insights for designing meaningful endpoints in clinical trials for durable

LVADs that could partially rely on the degree of CNS structural integrity before intervention, considering highly relevant contextual factors such as age, cardiomyopathy etiology, sex, and INTERMACS profile.

Conclusions

The use of clinical non-contrast CT brain imaging is a promising tool for assessing the risk of postoperative delirium. New-generation processing pipelines can enrich and augment imaging data, offering a feasible alternative when contrast high-resolution CT or conventional MRI is contraindicated. The findings suggest that significant brain parenchymal loss, not attributable to gray or white matter atrophy at the time of LVAD implantation, may drive the incidence of neurological dysfunction in patients with ADHF undergoing LVAD. However, these results should be replicated in a multicenter validation study. These and future insights are considered to be crucial for designing future studies to assess the risk of neurological dysfunction in patients undergoing durable MCS.

Data availability

The datasets used and/or analyzed during the present study are available from the corresponding author upon reasonable request. All data generated or analyzed during this study are included in this published article [and its supplementary information file].

Received: 8 December 2024; Accepted: 11 March 2025
Published online: 14 March 2025

References

1. Truby, L. K. & Rogers, J. G. Advanced heart failure: Epidemiology, diagnosis, and therapeutic approaches. *JACC Heart Fail.* **8**, 523–536. https://doi.org/10.1016/j.jchf.2020.01.014 (2020).
2. Han, J. J., Acker, M. A. & Atluri, P. Left ventricular assist devices: synergistic model between technology and medicine. Circulation*Circulation* **138**, 2841–2851, doi:https://doi.org/10.1161/circulationaha.118.035566 (2018).
3. Mullan, C. W. et al. Changes in use of left ventricular assist devices as Bridge to transplantation with new heart allocation policy. *JACC Heart Fail.* **9**, 420–429. https://doi.org/10.1016/j.jchf.2021.01.010 (2021).
4. Truby, L. K. et al. Ventricular assist device utilization in heart transplant candidates: nationwide variability and impact on waitlist outcomes. *Circ. Heart Fail.* **11**, e004586. https://doi.org/10.1161/circheartfailure.117.004586 (2018).
5. Thompson, M. P. et al. Center variation in medicare spending for durable left ventricular assist device implant hospitalizations. *JAMA Cardiol.* **4**, 153–160. https://doi.org/10.1001/jamacardio.2018.4717 (2019).
6. Pagani, F. D. et al. Clinical outcomes and healthcare expenditures in the real world with left ventricular assist devices - The CLEAR-LVAD study. *J. Heart Lung Transpl.* **40**, 323–333. https://doi.org/10.1016/j.healun.2021.02.010 (2021).
7. STS Intermacs Site Users. Guide Version 6.1. Appendix A – Adverse Event Definitions. University of Alabama at Birmingham. (2023). Available at: https://intermacs.kirso.net/intermacs-documents/ Accessed on August 18.
8. Hernandez, N. S. et al. Radiographic risk factors for intracranial hemorrhage in patients with left ventricular assist devices. *J. Stroke Cerebrovasc. Dis.* **31**, 106869. https://doi.org/10.1016/j.jstrokecerebrovasdis.2022.106869 (2022).
9. Kawabori, M. et al. Fatal neurologic dysfunction during Continuous-Flow left ventricular assist device support. *Ann. Thorac. Surg.* **107**, 1132–1138. https://doi.org/10.1016/j.athoracsur.2018.10.012 (2019).
10. Izzy, S. et al. Cerebrovascular accidents during mechanical circulatory support: New predictors of ischemic and hemorrhagic strokes and outcome. *Stroke* **49**, 1197–1203. https://doi.org/10.1161/strokeaha.117.020002 (2018).
11. Acharya, D. et al. INTERMACS analysis of stroke during support with continuous-flow left ventricular assist devices: risk factors and outcomes. *JACC Heart Fail.* **5**, 703–711. https://doi.org/10.1016/j.jchf.2017.06.014 (2017).
12. Harvey, L. et al. Stroke after left ventricular assist device implantation: outcomes in the Continuous-Flow era. *Ann. Thorac. Surg.* **100**, 535–541. https://doi.org/10.1016/j.athoracsur.2015.02.094 (2015).
13. Ibeh, C., Melmed, K. R., Yuzefpolskaya, M., Colombo, P. C. & Willey, J. Z. Stroke epidemiology and outcomes in the modern era of left ventricular assist devices. *Heart Fail. Rev.* **27**, 393–398. https://doi.org/10.1007/s10741-021-10201-x (2022).
14. Plecash, A. R., Byrne, D., Flexman, A., Toma, M. & Field, T. S. Stroke in patients with left ventricular assist devices. *Cerebrovasc. Dis.* **51**, 3–13. https://doi.org/10.1159/000517454 (2022).
15. Cho, S. M., Moazami, N. & Frontera, J. A. Stroke and intracranial hemorrhage in heartmate II and heartware left ventricular assist devices: A systematic review. *Neurocrit Care.* **27**, 17–25. https://doi.org/10.1007/s12028-017-0386-7 (2017).
16. Giray, S. et al. Does stroke etiology play a role in predicting outcome of acute stroke patients who underwent endovascular treatment with stent retrievers? *J. Neurol. Sci.* **372**, 104–109. https://doi.org/10.1016/j.jns.2016.11.006 (2017).
17. Kitano, T. et al. Mechanical thrombectomy in acute ischemic stroke patients with left ventricular assist device. *J. Neurol. Sci.* **418**, 117142. https://doi.org/10.1016/j.jns.2020.117142 (2020).
18. Pavol, M. A. et al. Cognition predicts days-alive-out-of-hospital after LVAD implantation. *Int. J. Artif. Organs.* **44**, 952–955. https://doi.org/10.1177/03913988211018484 (2021).
19. Noly, P. E. et al. Association of days alive and out of the hospital after ventricular assist device implantation with adverse events and quality of life. *JAMA Surg.* **158**, e228127. https://doi.org/10.1001/jamasurg.2022.8127 (2023).
20. Gazda, A. J. et al. Complications of LVAD utilization in older adults. *Heart Lung.* **50**, 75–79. https://doi.org/10.1016/j.hrtlng.2020.07.009 (2021).
21. Brown, C. H. et al. The association of brain MRI characteristics and postoperative delirium in cardiac surgery patients. *Clin. Ther.* **37**, 2686–2699e2689. https://doi.org/10.1016/j.clinthera.2015.10.021 (2015).
22. Kant, I. M. J. et al. Postoperative delirium is associated with grey matter brain volume loss. *Brain Commun.* **5**, fcad013. https://doi.org/10.1093/braincomms/fcad013 (2023).
23. Sprung, J. et al. Brain MRI after critical care admission: A longitudinal imaging study. *J. Crit. Care.* **62**, 117–123. https://doi.org/10.1016/j.jcrc.2020.11.024 (2021).
24. Saczynski, J. S. et al. Cognitive and brain reserve and the risk of postoperative delirium in older patients. *Lancet Psychiatry.* **1**, 437–443. https://doi.org/10.1016/s2215-0366(14)00009-1 (2014).
25. Cavallari, M. et al. Brain atrophy and white-matter hyperintensities are not significantly associated with incidence and severity of postoperative delirium in older persons without dementia. *Neurobiol. Aging.* **36**, 2122–2129. https://doi.org/10.1016/j.neurobiolaging.2015.02.024 (2015).
26. Fislage, M. et al. Presurgical thalamus volume in postoperative delirium: A longitudinal observational cohort study in older patients. *Anesth. Analg.* **135**, 136–142. https://doi.org/10.1213/ane.0000000000005987 (2022).
27. Fislage, M. et al. Presurgical diffusion metrics of the thalamus and thalamic nuclei in postoperative delirium: A prospective two-centre cohort study in older patients. *Neuroimage Clin.* **36**, 103208. https://doi.org/10.1016/j.nicl.2022.103208 (2022).

28. Fislage, M. et al. Preoperative thalamus volume is not associated with preoperative cognitive impairment (preCI) or postoperative cognitive dysfunction (POCD). *Sci. Rep.* **13**, 11732. https://doi.org/10.1038/s41598-023-38673-x (2023).
29. Gunther, M. L. et al. The association between brain volumes, delirium duration, and cognitive outcomes in intensive care unit survivors: the VISIONS cohort magnetic resonance imaging study*. *Crit. Care Med.* **40**, 2022–2032. https://doi.org/10.1097/CCM.0b013e318250acc0 (2012).
30. Beck, D. et al. Cardiometabolic risk factors associated with brain age and accelerate brain ageing. *Hum. Brain Mapp.* **43**, 700–720. https://doi.org/10.1002/hbm.25680 (2022).
31. Wood, D. A. et al. Accurate brain-age models for routine clinical MRI examinations. *Neuroimage* **249**, 118871. https://doi.org/10.1016/j.neuroimage.2022.118871 (2022).
32. Suzuki, H. et al. Associations of regional brain structural differences with aging, modifiable risk factors for dementia, and cognitive performance. *JAMA Netw. Open.* **2**, e1917257. https://doi.org/10.1001/jamanetworkopen.2019.17257 (2019).
33. Dekkers, I. A., Jansen, P. R., Lamb, H. J. & Obesity Brain volume, and white matter microstructure at MRI: A Cross-sectional UK biobank study. *Radiology* **291**, 763–771. https://doi.org/10.1148/radiol.2019181012 (2019).
34. Morys, F. et al. Obesity-Associated neurodegeneration pattern mimics Alzheimer's disease in an observational cohort study. *J. Alzheimers Dis.* **91**, 1059–1071. https://doi.org/10.3233/jad-220535 (2023).
35. De Luca, A., Kuijf, H., Exalto, L., Thiebaut de Schotten, M. & Biessels, G. J. Multimodal tract-based MRI metrics outperform whole brain markers in determining cognitive impact of small vessel disease-related brain injury. *Brain Struct. Funct.* **227**, 2553–2567. https://doi.org/10.1007/s00429-022-02546-2 (2022).
36. Bretzner, M. et al. Radiomics-Derived brain age predicts functional outcome after acute ischemic stroke. *Neurology* **100**, e822–e833. https://doi.org/10.1212/wnl.0000000000201596 (2023).
37. American Psychiatric. *Association. (2022). Diagnostic and statistical manual of mental disorders (5th ed., text rev.).* https://doi.org/10.1176/appi.books.9780890425787
38. Maldonado, J. R. et al. The Stanford integrated psychosocial assessment for transplantation (SIPAT): a new tool for the psychosocial evaluation of pre-transplant candidates. *Psychosomatics* **53**, 123–132. https://doi.org/10.1016/j.psym.2011.12.012 (2012).
39. Hamadnalla, H. et al. Optimal interval and duration of CAM-ICU assessments for delirium detection after cardiac surgery. *J. Clin. Anesth.* **71**, 110233. https://doi.org/10.1016/j.jclinane.2021.110233 (2021).
40. Saczynski, J. S. et al. A Tale of two methods: Chart and interview methods for identifying delirium. *J. Am. Geriatr. Soc.* **62**, 518–524. https://doi.org/10.1111/jgs.12684 (2014).
41. Kaffenberger, T. et al. Stroke population-specific neuroanatomical CT-MRI brain atlas. *Neuroradiology* **64**, 1557–1567. https://doi.org/10.1007/s00234-021-02875-9 (2022).
42. Billot, B. et al. Segmentation of brain MRI scans of any contrast and resolution without retraining. *Med. Image Anal.* **86**, 102789. https://doi.org/10.1016/j.media.2023.102789 (2023). SynthSeg.
43. Gorczowski, K. et al. Multi-object analysis of volume, pose, and shape using statistical discrimination. *IEEE Trans. Pattern Anal. Mach. Intell.* **32**, 652–661. https://doi.org/10.1109/tpami.2009.92 (2010).
44. Tafelmeier, M. et al. Predictors of delirium after cardiac surgery in patients with sleep disordered breathing. *Eur. Respir J.* **54** https://doi.org/10.1183/13993003.00354-2019 (2019).
45. Kirfel, A. et al. Postoperative delirium after cardiac surgery of elderly patients as an independent risk factor for prolonged length of stay in intensive care unit and in hospital. *Aging Clin. Exp. Res.* **33**, 3047–3056. https://doi.org/10.1007/s40520-021-01842-x (2021).
46. Smulter, N., Lingehall, H. C., Gustafson, Y., Olofsson, B. & Engström, K. G. Delirium after cardiac surgery: Incidence and risk factors. *Interact. Cardiovasc. Thorac. Surg.* **17**, 790–796. https://doi.org/10.1093/icvts/ivt323 (2013).
47. Raats, J. W., van Eijsden, W. A., Crolla, R. M., Steyerberg, E. W. & van der Laan, L. Risk factors and outcomes for postoperative delirium after major surgery in elderly patients. *PLoS One.* **10**, e0136071. https://doi.org/10.1371/journal.pone.0136071 (2015).
48. Smith, T. O. et al. Factors predicting incidence of post-operative delirium in older people following hip fracture surgery: a systematic review and meta-analysis. *Int. J. Geriatr. Psychiatry.* **32**, 386–396. https://doi.org/10.1002/gps.4655 (2017).
49. Duering, M. et al. Neuroimaging standards for research into small vessel disease-advances since 2013. *Lancet Neurol.* **22**, 602–618. https://doi.org/10.1016/s1474-4422(23)00131-x (2023).
50. Omiya, H. et al. Preoperative brain magnetic resonance imaging and postoperative delirium after off-pump coronary artery bypass grafting: a prospective cohort study. *Can. J. Anaesth.* **62**, 595–602. https://doi.org/10.1007/s12630-015-0327-x (2015).
51. Lascola, C. D. et al. Blood-brain barrier permeability and cognitive dysfunction after surgery - A pilot study. *J. Clin. Anesth.* **86**, 111059. https://doi.org/10.1016/j.jclinane.2023.111059 (2023).
52. Okamura, T., Ishibashi, N., Zurakowski, D. & Jonas, R. A. Cardiopulmonary bypass increases permeability of the blood-cerebrospinal fluid barrier. *Ann. Thorac. Surg.* **89**, 187–194. https://doi.org/10.1016/j.athoracsur.2009.09.030 (2010).
53. Vasunilashorn, S. M. et al. Plasma and cerebrospinal fluid inflammation and the blood-brain barrier in older surgical patients: the role of inflammation after surgery for elders (RISE) study. *J. Neuroinflammation.* **18**, 103. https://doi.org/10.1186/s12974-021-02145-8 (2021).
54. Merino, J. G. et al. Blood-brain barrier disruption after cardiac surgery. *AJNR Am. J. Neuroradiol.* **34**, 518–523. https://doi.org/10.3174/ajnr.A3251 (2013).
55. Freeze, W. M. et al. CSF enhancement on post-contrast fluid-attenuated inversion recovery images; a systematic review. *Neuroimage Clin.* **28**, 102456. https://doi.org/10.1016/j.nicl.2020.102456 (2020).
56. Medicare program; criteria for. Medicare coverage of heart transplants–HCFA. Notice of HCFA ruling. *Fed. Regist.* **52**, 10935–10951 (1987).
57. Chen, H., Mo, L., Hu, H., Ou, Y. & Luo, J. Risk factors of postoperative delirium after cardiac surgery: a meta-analysis. *J. Cardiothorac. Surg.* **16**, 113. https://doi.org/10.1186/s13019-021-01496-w (2021).
58. Dempsey, R. J. et al. Carotid atherosclerotic plaque instability and cognition determined by ultrasound-measured plaque strain in asymptomatic patients with significant stenosis. *J. Neurosurg.* **128**, 111–119. https://doi.org/10.3171/2016.10.Jns161299 (2018).
59. Fiamanya, S., Ma, S. & Yates, D. R. A. The association between preoperative Mini-Cog© score and postoperative delirium (POD): A retrospective cohort study. *Perioper Med. (Lond).* **11**, 16. https://doi.org/10.1186/s13741-022-00249-0 (2022).
60. Susano, M. J. et al. Brief preoperative screening for frailty and cognitive impairment predicts delirium after spine surgery. *Anesthesiology* **133**, 1184–1191. https://doi.org/10.1097/aln.0000000000003523 (2020).
61. Weiss, Y. et al. Preoperative cognitive impairment and postoperative delirium in elderly surgical patients: A retrospective large cohort study (The CIPOD study). *Ann. Surg.* **278**, 59–64. https://doi.org/10.1097/sla.0000000000005657 (2023).
62. Yuzefpolskaya, M. et al. The society of thoracic surgeons intermacs 2022 annual report: focus on the 2018 heart transplant allocation system. *Ann. Thorac. Surg.* **115**, 311–327. https://doi.org/10.1016/j.athoracsur.2022.11.023 (2023).

Author contributions

This study was conceptualized by IMA and NKM. IMA, JMB, JPS, JU, ZX, and GZ collected and analyzed the data. IMA, NKM and JMB discussed and interpreted the results. IMA and NKM drafted the manuscript. IMA, NKM, SL, VB, CPW, AES, CHM, TKR, and KKL provided significant conceptual contributions and reviewed the manuscript. All authors read and approved the final manuscript. NKM conceived the project, received funding, and supervised the project.

Funding
Baylor College of Medicine Faculty Research Grant, Baylor College of Medicine Interdisciplinary Surgical Technology and Innovation Center (INSTINCT), and Rice University Educational and Research Initiatives for Collaborative Health (ENRICH) grants to Dr. Mondal.

Declarations

Competing interests
The authors declare no competing interests.

Additional information
Supplementary Information The online version contains supplementary material available at https://doi.org/10.1038/s41598-025-94074-2.

Correspondence and requests for materials should be addressed to N.K.M.

Reprints and permissions information is available at www.nature.com/reprints.

Publisher's note Springer Nature remains neutral with regard to jurisdictional claims in published maps and institutional affiliations.